# A gas-transport model predicts the *Arabidopsis* spaceflight transcriptome, and illumination separates six flight contrasts

Richard Barker[1*]

[1]Independent researcher, [TODO], [TODO].

Corresponding author(s). E-mail(s): dr.richard.barker@gmail.com;

**Abstract**

Plants flown on the International Space Station are grown inside enclosures, and the atmosphere inside those enclosures is rarely measured. We coupled a validated lattice-Boltzmann model of leaf boundary-layer gas transport to a Farquhar–von Caemmerer–Berry model of $C_3$ photosynthesis and asked what an illuminated, sealed canister does to the $CO_2$ reaching Rubisco. A mass balance with an assumed headspace predicts that photosynthesis draws a sealed Biological Research in Canisters (BRIC) enclosure toward its $CO_2$ compensation point within minutes, reducing 12 h carbon gain to 1 % of an unenclosed control; at a drawn-down 100 ppm, an assumed value, the Rubisco oxygenation fraction rises from 28 % to 54 % at saturating light. Because that drawdown is a mass balance, it occurs in the ground control as well as in flight. It therefore does not bias the flight-versus-ground contrast every such experiment reports — it changes what that contrast is *about*. We estimate the enclosure effect on metabolite pools to be 22 times the microgravity effect, which means the spaceflight response is being measured in plants their own hardware has already carbon-starved. Contrary to our own starting hypothesis, the microgravity boundary-layer penalty does not amplify as $CO_2$ falls; it converges, leaving a persistent assimilation deficit at saturating light of 5–9 % at leaf and rosette scale and 26–29 % in a dense canopy, and under 3 % at leaf and rosette scale at the experiment's own light level. We tested these predictions against OSD-522 (BRIC-LED), where the model called eight of nine transcriptome gene-set responses and four of seven in the proteome, and against four further OSDR studies, six flight-versus-ground contrasts in all. On the starvation-over-photosynthesis contrast illumination separated the six completely — every illuminated contrast positive, every dark one negative, although the model predicted no signal in the dark rather than an inverse — while the predicted gradient across enclosure types did not hold. NASA's Open Science Data

Repository contains no plant metabolome at all (none of its twelve metabolite-profiling studies is of a plant), so the third omic layer for pathway integration had to be predicted rather than measured. We argue that enclosure atmosphere is a first-order, currently unmeasured covariate in plant spaceflight biology — not a bias to correct for, but a baseline state to measure — and set out the three-arm design and the in-canister measurement that would establish it.

**Keywords:** spaceflight, microgravity, photorespiration, *Arabidopsis*, growth hardware, multi-omics

# 1 Introduction

Interpreting a plant spaceflight experiment means attributing a molecular difference to microgravity. That attribution rests on an assumption that is almost never tested: that the flight and ground arms differ in gravity and in nothing else that matters to metabolism.

Plants flown on the International Space Station are grown inside enclosures — sealed Petri Dish Fixation Units in BRIC canisters, Petri plates on the cabin wall in CARA, actively ventilated chambers in VEGGIE and the Advanced Plant Habitat. These enclosures differ by orders of magnitude in how freely they exchange gas with the cabin, and to our knowledge no BRIC-class flight has logged the $CO_2$ concentration its plants actually experienced.

The quantity that matters is not the cabin atmosphere but the $CO_2$ mole fraction reaching Rubisco, $C_c$, which sits at the end of a chain of conductances: from bulk air across the leaf boundary layer, through the stomata, and through the mesophyll. Only the first of those is gravity-dependent, through buoyancy-driven convection. Rubisco partitions between carboxylation and oxygenation as $V_o/V_c = 2\Gamma^*/C_c$ [1], so anything that lowers $C_c$ raises photorespiration.

Here we ask a question about the enclosure rather than about gravity, and we ask it of the model before we ask it of any data.

# 2 Results

## 2.1 An illuminated sealed canister is a $CO_2$-starvation chamber

Boundary-layer conductance was taken from LunarLeaf-CFD [2], a lattice-Boltzmann solver validated against four analytical and empirical gates. The enclosure figures come from two simpler models in the same repository, not from that solver. A headspace mass balance, with an assumed 30 mL of air over 3 $cm^2$ of leaf, draws a lit BRIC canister from 400 ppm to near zero in approximately seven minutes; a zero-dimensional photosynthesis-feedback model puts 12 h carbon gain at 1 % of an unenclosed 1 $g$ control, against 90 % for a dish sealed with gas-permeable tape of assumed permeance and 100 % when ventilated (Fig. 1).

The step that matters for interpretation is that this drawdown is a mass balance between photosynthetic uptake and enclosure volume. It is therefore essentially gravity-independent, and it happens in the ground control as much as in flight.

## 2.2 What that does to Rubisco, and what gravity does not do

Feeding the boundary-layer conductance into a Farquhar–von Caemmerer–Berry model [1] with in-vivo Rubisco kinetics [3, 4], solved at saturating irradiance (1,000 µmol $m^{-2}\,s^{-1}$), moves the leaf along its $CO_2$ response curve: oxygenation fraction rises from 28.5 % in ventilated hardware at ambient $CO_2$ to 53.7 % in a drawndown canister (Fig. 2a, Table 1). The canister value is an assumption: the sealed arms are placed at 100 ppm, whereas at this light the compensation point is 54 ppm, where the fraction would be 61 %.

We began from the hypothesis that $CO_2$ starvation would *amplify* the microgravity boundary-layer penalty. The model says the opposite (Fig. 2b). As assimilation falls toward the compensation point, the flux through the boundary layer falls with it, so the $CO_2$ drop across that layer, $A/g_{bl}$, tends to zero and the two gravities converge. What survives is a persistent proportional assimilation deficit of 5–7 % at leaf scale, 7–9 % at rosette scale and 26–29 % in a dense canopy, nearly independent of where in the drawdown the plant sits (Fig. 2c). That insensitivity is the prediction's strength: it does not require knowing the canister $CO_2$, which nobody measured. Both the size of the deficit and its insensitivity hold at saturating light only; at the light level of the experiments tested below the deficit is smaller and does depend on $CO_2$ (see Limitations).

Propagating both contrasts to metabolite pools makes the asymmetry explicit. The sealed-versus-ventilated hardware effect is 22 times the flight-versus-ground effect (Fig. 2d) — and because it acts on both arms, it cancels.

## 2.3 A metabolite layer that does not exist

Pathway-level integration needs a metabolome. We queried all 567 OSDR studies and cross-tabulated organism against assay type: twelve are metabolite profiling, and every one is mouse, human, rat or microbial. **No plant study has a metabolome.**

We therefore predicted one (Fig. 3), propagating the modelled fluxes to 21 compounds under one stated assumption — that at quasi-steady state a pool tracks the flux feeding it. Every value is labelled as model output in every file. Compounds the model cannot speak to, including all tricarboxylic-acid intermediates and all fermentation products, are excluded with the reason recorded rather than filled in.

## 2.4 The model called eight of nine transcriptome gene sets

OSD-522 [5] grew *Arabidopsis* in BRIC-LED hardware under 60 µmol $m^{-2}\,s^{-1}$ of red and blue light, with six flight and six ground-control shoot samples. We computed differential expression with PyDESeq2 [6], obtaining 1,795 genes at FDR $< 0.05$ from 19,325 with an adjusted $p$ (20,983 measured), and used the deposited proteomics ratios for 5,160 proteins (Fig. 4).

Scoring these against KEGG-derived gene sets (Fig. 5), the model's predictions held for eight of nine sets: the photosystem and light-harvesting apparatus fell ($-0.238$, $p = 3.8 \times 10^{-6}$; and in the proteome $-0.820$, $p = 5.0 \times 10^{-4}$), Rubisco fell ($-0.403$, $p = 4.5 \times 10^{-3}$), carbon fixation and starch/sucrose metabolism fell, carbon-starvation DIN markers rose ($+0.685$, $p = 2.6 \times 10^{-3}$), and photorespiratory enzymes were not induced. The one mismatch is the whole KEGG glyoxylate and dicarboxylate map, which contains a good deal besides the $C_2$ cycle. Three of the eight matches are sets predicted not to change, which pass by not reaching $p < 0.05$, on three to thirteen genes each. In the proteome the predictions held for four of seven testable sets: carbon fixation, starch/sucrose and Rubisco did not fall significantly.

The sharper test is between sets, which is immune to the global depression of metabolic transcripts: photorespiratory enzymes sat above Rubisco in the transcriptome ($+0.239$, $p = 6.8 \times 10^{-3}$) and independently in the proteome ($+0.285$, $p = 4.9 \times 10^{-2}$). The third set-versus-set test, photorespiration against carbon fixation as whole KEGG maps, showed no signal in either layer ($-0.020$, $p = 0.95$; $+0.030$, $p = 0.82$).

## 2.5 Pathway integration puts photorespiration in the bottom 8 %

Submitting all three layers to PaintOmics [7] against KEGG and MapMan (Fig. 6), 97–100 % of genes, 97 % of proteins and all 21 predicted compounds mapped. Of 232 pathways tested, 32 reached combined Fisher $p < 0.05$ uncorrected, including photosynthesis ($p = 0.008$), photosynthesis antenna proteins ($p = 0.022$) and starch and sucrose metabolism ($p = 0.019$). Six survive Benjamini–Hochberg correction at FDR $< 0.05$, led by protein processing in the endoplasmic reticulum, and none of the pathways the model made a claim about is among them (photosynthesis FDR $= 0.14$). Glyoxylate and dicarboxylate metabolism — the photorespiration map — ranked *214th of 232* at $p = 0.994$, in the bottom 8 % and the least enriched of any pathway the model made a claim about. Eighteen pathways rank below it, nine of them at $p = 1$.

The metabolite hub analysis is the least circular result available here, because the compounds are predicted but the differentially expressed genes counted around them are measured. Fifteen compounds entered it: the thirteen submitted as changed, and two glucose anomers onto which PaintOmics also mapped D-glucose. Seven reached FDR $< 0.05$, and every one was a carbon-starvation or carbon-supply node. The eight $C_2$ photorespiratory intermediates were not submitted as changed, because the model predicted almost no change in them ($\log_2$FC 0.003), and none entered the hub analysis, so it says nothing about them.

## 2.6 Illumination separates six contrasts; the enclosure gradient does not

The model's claim is an ordering, so we tested it across six matched flight-versus-ground contrasts from five studies, spanning three enclosure classes [8–11]; OSD-678 contributes a lit and a dark arm (Fig. 7; selection and exclusions in Table 2).

On the starvation-over-photosynthesis contrast, illumination separated them completely: all three illuminated contrasts were positive (+0.41, +0.92, +2.58) and all three dark ones negative (−0.39, −1.95, −3.22); one-sided Mann–Whitney $p = 0.05$, the floor attainable at three versus three. The model predicted no signal in the dark, not an inverse, and the significant inversions in the two BRIC-PDFU studies are unexplained. In OSD-678's dark arm the starvation markers still rose (+2.07, $p = 0.007$); its negative value comes from photosystem genes rising further, and is not significant ($p = 0.12$). The separation is not complete on every contrast: on photorespiration against carbon fixation, OSD-678's dark arm sits above every lit one. The cleanest evidence is internal: OSD-678 light (+2.58) against OSD-678 dark (−0.39) is the same hardware, genotype and flight. Two further caveats bear on the illumination reading. OSD-38's dark condition is inferred from its hardware rather than stated, and OSD-678's lit arm grew in diffuse cabin light of 4–6 µmol $m^{-2}\,s^{-1}$, an order of magnitude below OSD-522, yet shows the strongest signature.

The predicted gradient across enclosure classes did *not* hold (Spearman $\rho = -0.50$, $p = 0.67$). Sealed and ventilated fell the right way round but the CARA plates, modelled as tape-sealed, sat highest, and three studies cannot rank three classes. We report this as a failure of that prediction. The driver appears to be illumination inside an enclosure rather than sealing as such — which is mechanistically what the model says, since drawdown requires photosynthesis to be running.

# 3 Discussion

The strongest signal in the OSD-522 integration is one this model does not explain: protein processing in the endoplasmic reticulum, at $p = 8.6 \times 10^{-9}$, the unfolded protein response. A gas-transport account explains part of this experiment, not all of it.

What the analysis does support is narrower and, we think, more useful. In an illuminated enclosure the atmosphere the plants experience is set by the hardware, it is not measured, and it is large. Because it acts on both arms it does not bias the published contrast — which is precisely why it has gone unnoticed. What it does instead is set the physiological state in which the microgravity response is read out: not a healthy plant, but a carbon-starved one. That is a baseline condition, not a bias to correct for, and a sensor would settle it.

## 3.1 Limitations

Cross-study comparison is the weakest joint here: different laboratories, durations, genotypes and harvest protocols. We restricted to GeneLab-standard RNA-seq, aerial tissue where a study offered it, and matched contrasts, and we report gene-set *ordering* rather than absolute effect sizes, but the limitation stands. Two of the three dark studies are whole seedlings, so tissue is partly confounded with illumination. The illumination result rests on three contrasts per group, from five studies. The predictions and the tests that score them entered the repository in the same commit, so the record cannot show that the predictions were fixed first. Pathway enrichment is reported at uncorrected $p$; after FDR correction six of 232 pathways remain, none of them one

the model made a claim about. The enclosure drawdown and carbon-gain figures rest on an assumed headspace volume and tape permeance, and OSDR does not describe how the CARA plates were sealed. The intended ventilated proteome arm does not exist, because OSD-16 has no processed files, so the two-layer comparison is confined to sealed hardware. The metabolite layer is predicted throughout, and the metabolite class-activity test is close to circular because it tests our own predicted list; the hub analysis is not, and is reported as the informative one. The photosynthesis model is solved at saturating irradiance, 1,000 µmol $m^{-2}$ $s^{-1}$, whereas OSD-522 was grown at 60. At 60 the same calculation puts the oxygenation fraction at 18 % in ventilated hardware at ambient $CO_2$ and 46 % at 100 ppm, which at that light is the compensation point, and the microgravity assimilation deficit at under 3 % at leaf and rosette scale and up to 11 % in a dense canopy, growing as $CO_2$ falls rather than holding flat. The direction of each prediction is unchanged, but the magnitudes in Table 1 and Fig. 2 are saturating-light values (`results/tables/T13_light_sensitivity.tsv`). Finally, $V_{cmax}$, $J_{max}$, $R_d$, $g_s$ and $g_m$ remain literature values for *Arabidopsis* rather than fits to flight material, and $g_s$ is held fixed although BRIC canisters are humid.

### 3.2 What would settle it

Three things, in increasing cost. First, log $CO_2$ and $O_2$ inside the canister: the central assumption of this analysis becomes a measurement, and an entire archive of BRIC-derived transcriptomes becomes reinterpretable. Second, run a targeted metabolite panel on archived flight material — roughly twenty compounds would be the first plant spaceflight metabolome in existence, and our predicted set is a ready-made target list. Third, fly a three-arm design (Fig. 8): flight sealed, ground sealed, ground ventilated. Two arms confound hardware with gravity; three separate them, and the third arm never leaves the ground.

## 4 Methods

Full methods, every script and every derived table are in the repository accompanying this manuscript. Study selection, including each exclusion and its reason, is in `data/study_registry.tsv`.

**Gas transport.** Boundary-layer conductance was taken from the lattice-Boltzmann solver in LunarLeaf-CFD [2], from its steady-state export (commit `e298785`, regenerated with `validation/export_cfd.ts`), and the enclosure drawdown time and 12 h carbon gain from its zero-dimensional models (`validation/hardware_analysis.py`, `validation/feedback_0d.py`), which assume a 30 mL dish headspace and a tape permeance; all were vendored into this repository.

**Photosynthesis model.** A Farquhar–von Caemmerer–Berry $C_3$ model [1] with the oxygenation term explicit, using in-vivo temperature responses [3, 4], solved for the supply-equals-demand operating point. Every operating point, assimilation deficit and metabolite prediction reported here is solved at an irradiance of 1,000 µmol $m^{-2}$ $s^{-1}$ (`scripts/fvcb.py`).

**Differential expression.** OSD-522 was processed with PyDESeq2 [6]. The other five studies use GeneLab's own deposited differential-expression tables, with matched flight-versus-ground contrasts selected by pattern and recorded in the registry.

**Gene sets.** Built from KEGG pathway membership and description regular expressions fetched live [12, 13], never typed from memory.

**Pathway integration.** PaintOmics [7], organism `ath`, KEGG and MapMan, with the optional AI interpretation disabled. The jobs were first run on a metabolite layer predicted from an earlier LunarLeaf-CFD export (photosynthate $\log_2$FC $-0.114$ against $-0.131$ now) and resubmitted on the current one; every pathway, per-omic and hub $p$-value was identical. PaintOmics reports enrichment but not the gene lists behind it, and MapMan has no equivalent of the KEGG REST API, so the gene membership used in the accompanying data explorer was reconstructed from GoMapMan's Araport11 gene-to-bin mapping and the MapMan diagram layouts, by PaintOmics' own inclusion rules. PaintOmics matches a diagram's bin codes anywhere in a gene's bin code, not only from the start, so its MapMan diagrams hold more than their names suggest: *photosynthesis* has 1,722 measured loci this way and 488 if matched from the start. It reproduces PaintOmics' feature count exactly or within three features for 9 of the 13 significant MapMan diagrams and runs larger for the four largest; both counts are reported rather than one, and the discrepancy on those four is not explained by any rule recoverable from PaintOmics' published sources.

## 4.1 Use of AI tools

The analysis code, figures and manuscript text were drafted with Claude Code (Anthropic), an AI coding assistant running Claude Opus models, working under the author's direction. Google Antigravity made figure-layout and website edits. The assistants also ran the checks that trace each reported number to the script output that produces it and match each reference against CrossRef or DataCite. The author directed the work, reviewed the results and takes full responsibility for the content.

**Supplementary information.** Supplementary Figure S1 places every locus in the significant pathways into its transcript and protein differential-expression bin, and reports how far the reconstructed MapMan membership agrees with PaintOmics' own feature counts.

**Data availability.** All primary data are public in the NASA Open Science Data Repository [14]: OSD-522, OSD-38, OSD-321, OSD-678 and OSD-427. Derived tables and figures are archived with this manuscript. TODO insert the Zenodo DOI on deposit.

**Code availability.** The analysis code is available at https://github.com/dr-richard-barker/Photorespiration_multiomics_microgravity. TODO insert the archived release DOI.

**Acknowledgements.** TODO.

**Author contributions.** R.B. is the sole author and takes responsibility for all of this work.

**Table 1** Modelled operating points at saturating light. Flight and ground control sit at effectively the same place because both are placed in a drawn-down canister, at an assumed 100 ppm; the ventilated arm is at ambient.

| Arm | $g_{bl}$ | $C_a$ | $C_c$ | $\varphi$ (%) | $A$ |
|---|---|---|---|---|---|
| Ground control (sealed) | 0.540 | 100 | 75.5 | 53.1 | 2.40 |
| Flight (sealed) | 0.272 | 100 | 73.6 | 53.7 | 2.20 |
| Ventilated (ambient) | 0.272 | 400 | 215.0 | 28.5 | 15.40 |

$g_{bl}$ in mol m$^{-2}$ s$^{-1}$; $C_a$ and $C_c$ in µmol mol$^{-1}$; $A$ in µmol m$^{-2}$ s$^{-1}$. Rosette scale.

**Table 2** The five studies analysed, giving six contrasts (OSD-678 has a lit and a dark arm), and the six excluded. Tissue is the binding constraint: a photosynthesis prediction says nothing about roots. CARA's enclosure class is modelled; OSDR describes Petri plates fixed to the cabin wall.

| Study | Hardware | Class | Tissue | Light |
|---|---|---|---|---|
| OSD-522 | BRIC-LED | sealed | shoots | lit |
| OSD-38 | BRIC-PDFU | sealed | whole seedlings | dark |
| OSD-321 | BRIC-PDFU | sealed | seedlings | dark |
| OSD-678 | CARA | tape | leaves | lit and dark |
| OSD-427 | VEGGIE | vented | leaf | lit |
| *Excluded:* OSD-120, OSD-193, OSD-281 (roots); OSD-218 (tissue unstated); OSD-16 (no processed files); OSD-7 (microarray, not comparable). | | | | |

**Funding.** This study received no funding.

**Competing interests.** The author declares no financial or non-financial competing interests.

# References

[1] Farquhar, G. D., von Caemmerer, S. & Berry, J. A. A biochemical model of photosynthetic $CO_2$ assimilation in leaves of $C_3$ species. *Planta* **149**, 78–90 (1980).

[2] Barker, R. LunarLeaf-CFD: a validated lattice-Boltzmann solver for leaf boundary-layer gas transport under variable gravity. https://github.com/dr-richard-barker/LunarLeaf-CFD. TODO cite the archived release DOI once deposited.

[3] Bernacchi, C. J., Singsaas, E. L., Pimentel, C., Portis Jr., A. R. & Long, S. P. Improved temperature response functions for models of Rubisco-limited photosynthesis. *Plant, Cell and Environment* **24**, 253–259 (2001).

[4] Bernacchi, C. J., Pimentel, C. & Long, S. P. In vivo temperature response functions of parameters required to model RuBP-limited photosynthesis. *Plant, Cell*

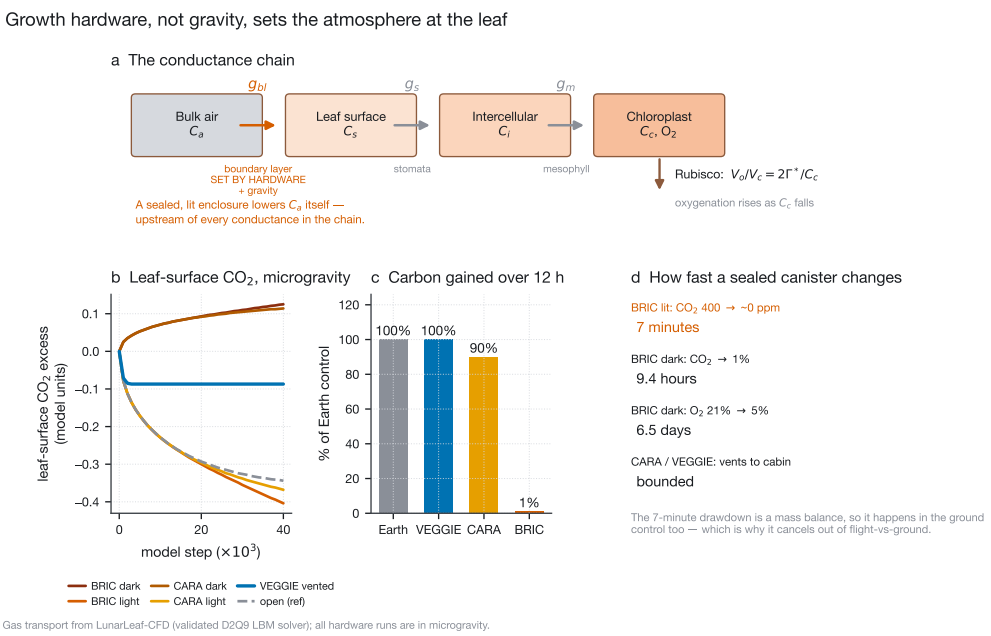



**Fig. 1** Growth hardware, not gravity, sets the atmosphere at the leaf. **b** shows $CO_2$ at the leaf surface, which is defined for all six cases and is the quantity the photosynthesis model consumes; the alternative series in the solver output, the mean over the enclosure volume, exists only for the four closed cases, because a vented enclosure has no closed volume to average.


*and Environment* **26**, 1419–1430 (2003).

[5] Integrative transcriptomics and proteomics profiling of *arabidopsis thaliana* elucidates novel mechanisms underlying spaceflight adaptation. NASA Open Science Data Repository, OSD-522 (BRIC-LED-001) (2024). https://osdr.nasa.gov/bio/repo/data/studies/OSD-522.

[6] Muzellec, B., Teleńczuk, M., Cabeli, V. & Andreux, M. PyDESeq2: a python package for bulk RNA-seq differential expression analysis. *Bioinformatics* **39**, btad547 (2023).

[7] Liu, T. *et al.* PaintOmics 4: new tools for the integrative analysis of multi-omics datasets supported by multiple pathway databases. *Nucleic Acids Research* **50**, W551–W559 (2022).

[8] Proteomics and transcriptomics analysis of *arabidopsis* seedlings in microgravity. NASA Open Science Data Repository, OSD-38 (BRIC-20) (2015). https://osdr.nasa.gov/bio/repo/data/studies/OSD-38.

[9] Relevance of unfolded protein response to spaceflight-induced transcriptional reprogramming in *arabidopsis*. NASA Open Science Data Repository, OSD-321 (BRIC-22) (2021). https://osdr.nasa.gov/bio/repo/data/studies/OSD-321.

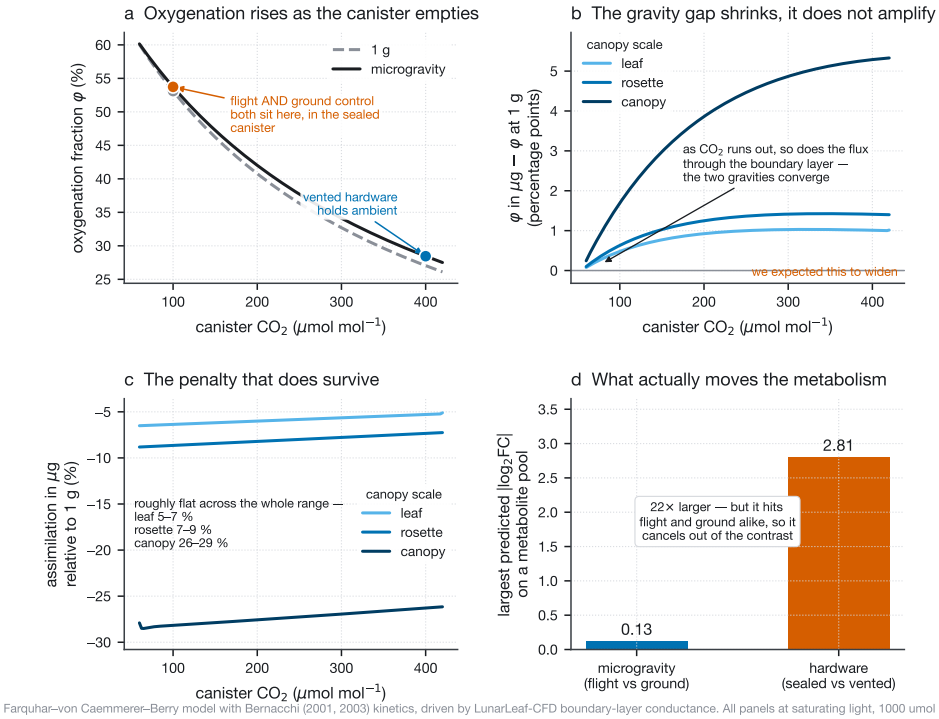



**Fig. 2** A drawn-down enclosure, not microgravity, is what reaches Rubisco. Panel b shows the refutation of our own starting hypothesis.


[10] Light has a principal role in the *arabidopsis* transcriptomic response to the spaceflight environment. NASA Open Science Data Repository, OSD-678 (CARA) (2023). https://osdr.nasa.gov/bio/repo/data/studies/OSD-678.

[11] Characterizing epigenetic changes in methylation mutants (*elp2-5* and *met1-7*) in response to spaceflight [RNA-Seq]. NASA Open Science Data Repository, OSD-427 (APEX-04) (2021). https://osdr.nasa.gov/bio/repo/data/studies/OSD-427.

[12] Kanehisa, M. & Goto, S. KEGG: Kyoto encyclopedia of genes and genomes. *Nucleic Acids Research* **28**, 27–30 (2000). Author list from PubMed (PMID 10592173); CrossRef and OpenAlex carry only the first author.

[13] KEGG: Kyoto encyclopedia of genes and genomes. https://www.kegg.jp/. Pathway membership and compound identifiers retrieved via the KEGG REST API, 8 September 2026.

[14] Gebre, S. G. *et al.* NASA open science data repository: open science for life in space. *Nucleic Acids Research* **53**, D1697–D1710 (2025). Online 2024-11-18; in print 2025-01-06 as volume 53 issue D1. Author list verified against CrossRef.

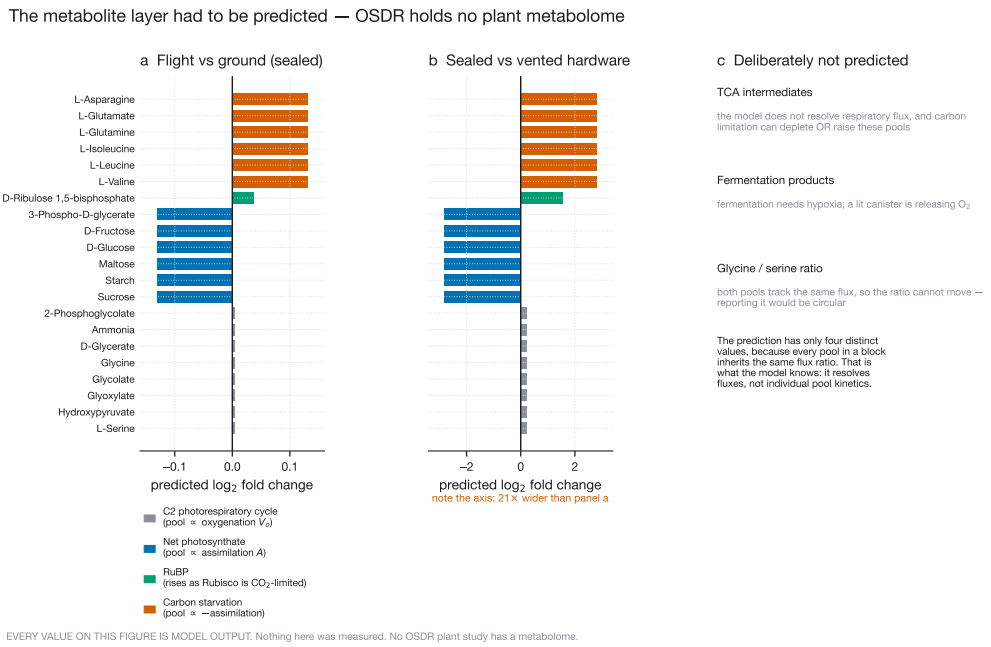



**Fig. 3** The metabolite layer had to be predicted. Every value shown is model output.

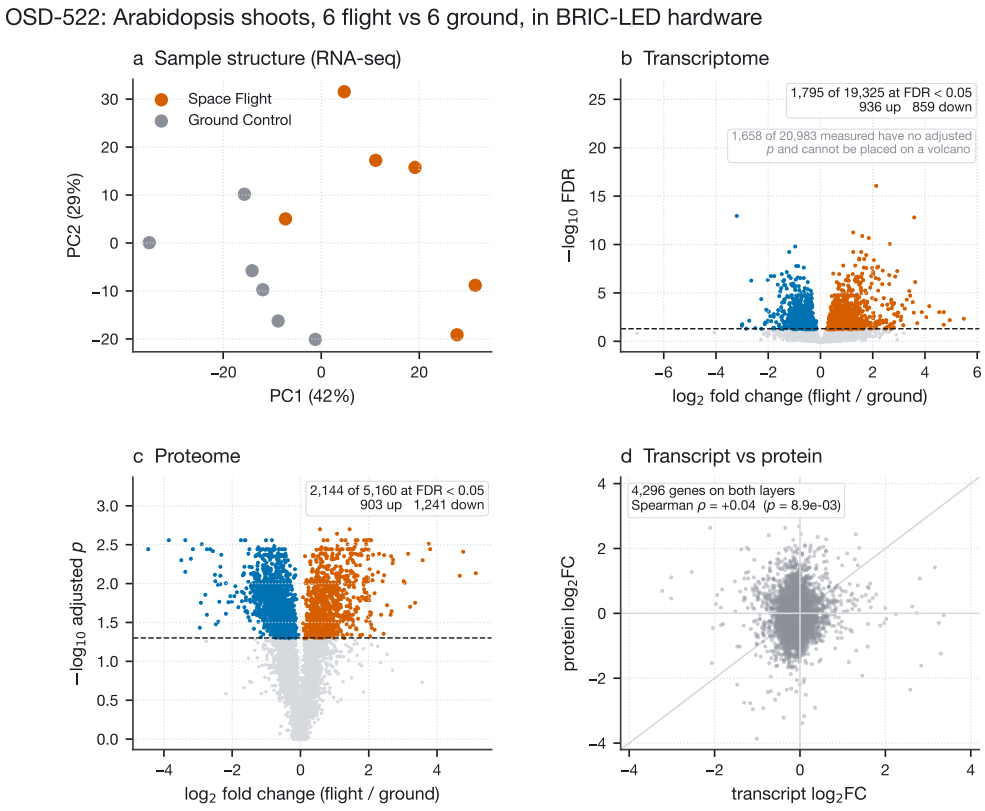



**Fig. 4** OSD-522: *Arabidopsis* shoots, six flight against six ground.

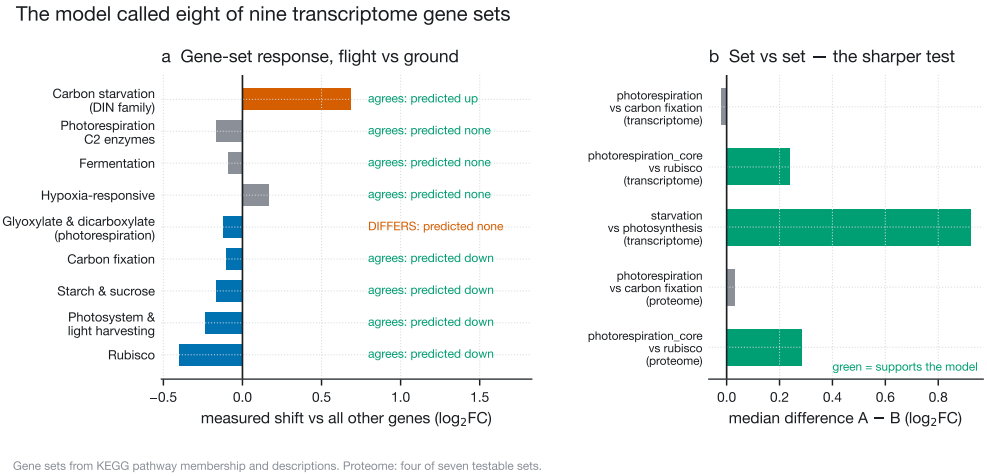



**Fig. 5** The model's prediction against the measurement.

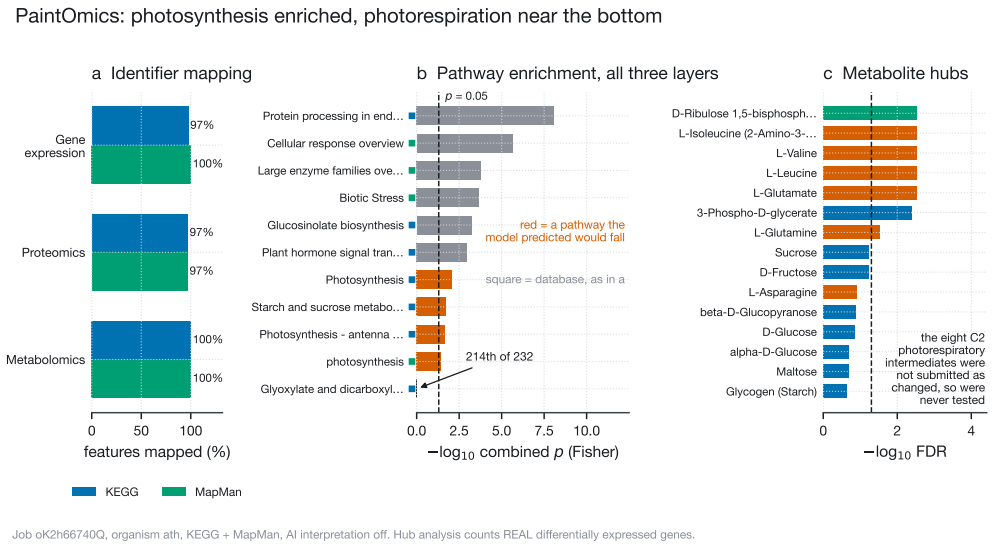



**Fig. 6** Pathway integration across all three layers. In **b** a square marks each pathway's database, in the colours of **a**: KEGG's *Photosynthesis* and MapMan's *photosynthesis* are different maps that differ only in capitalisation, and both reach uncorrected $p < 0.05$; neither survives FDR correction. MapMan's diagram, as PaintOmics resolves it, holds 1,722 measured loci against 488 in the photosynthesis bins themselves (Methods).

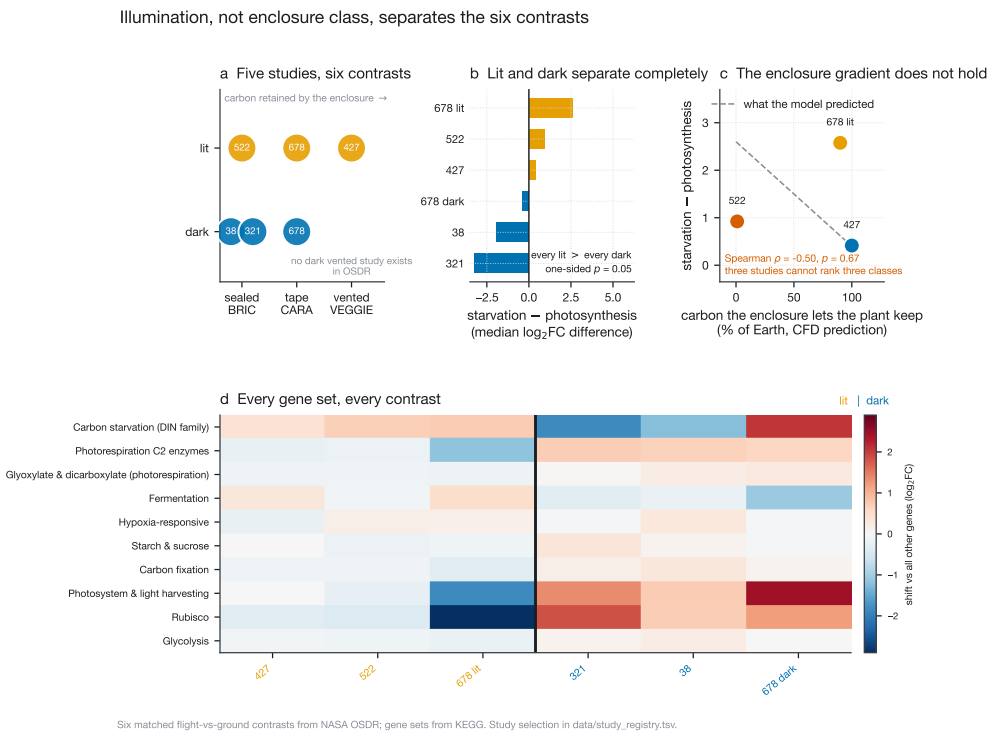



**Fig. 7** Illumination separates the six contrasts on starvation over photosynthesis; the enclosure gradient does not.

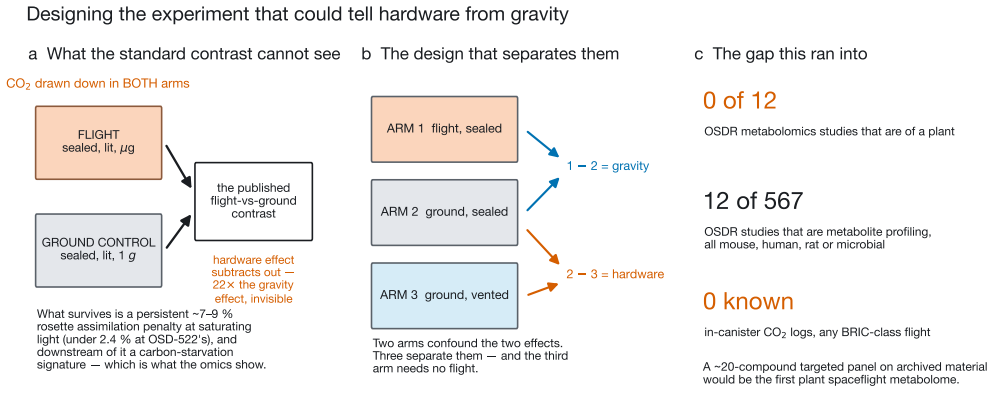



**Fig. 8** Designing the experiment that could tell hardware from gravity.